Surface Products and Coverage Dependence of Dissociative Ethane Adsorption on Pt{110}-(1 × 2)

J. J. W. Harris,[†] V. Fiorin,[†] C. T. Campbell,[‡] and D. A. King*,[†]

Department of Chemistry, University of Cambridge, Lensfield Road, Cambridge, CB2 1EW United Kingdom, and Chemistry Department, University of Washington, Seattle, Washington 98195-1700

Received: October 6, 2004; In Final Form: December 3, 2004

The dissociation of ethane on Pt{110}-(1 × 2) has been studied using supersonic molecular beam and temperature-programmed reaction techniques. The study unequivocally shows that the stable dissociation product of ethane on Pt{110}-(1 × 2) at all coverages is CCH_2 at 350−400 K and CCH at 440 K. Temperature-programmed-reaction (TPR) experiments indicate that the CCH_2 species decomposes to CCH with a reaction-limited peak temperature of 430 K. Above 450 K, the CCH species becomes unstable and decomposes with a peak temperature of 540 K. By 600 K, ethane dehydrogenates completely to form a surface carbon layer. The sticking probability is initially 0.02 at 370 K and 0.03 at 600 K and follows a linear $(1-2\theta)$ dependence for coverages of up to $\theta = 0.4$ ML, where θ is defined as the number of C_2H_x units per (1 × 2) unit cell. However, a much weaker coverage dependence at 800 K suggests that the carbon agglomerates into high-density islands.

1. Introduction

The identification of C_2 hydrocarbon fragments on metal surfaces is crucial in understanding a number of important catalytic processes, including alkene hydrogenation,[1] the catalytic steam cracking of ethane,[2] and the Fischer−Tropsch synthesis.[3,4] However, the chemistry of C_2 surface species is complex, and as a result of its importance and complexity, it has been studied extensively. Because ethylene and acetylene adlayers adsorb readily on metal surfaces, C_2H_x adlayers are frequently prepared from these species. Therefore, the adsorption and surface chemistry of ethylene have been studied on numerous single-crystal metal surfaces,[5−15] including platinum surfaces.[16−33] In contrast, there have been far fewer studies of the surface species and surface chemistry that arise from ethane adsorption on transition metal surfaces. This is because the dissociation probability of saturated hydrocarbons on platinum and other metal surfaces is typically very low,[34] although it can be increased to >0.01 using high energy molecular beams.[35−37] However, ethane adsorption and decomposition have been studied on Pt{111}.[38,39] Below 200 K, the ethyl (C_2H_5) surface species was found to be stable. The C_2H_5 species decomposed to $CHCH_3$ at $T_S = 250$ K in the presence of coadsorbed H_a and decomposed to ethylidyne, CCH_3, above 300 K.

The dissociative adsorption of methane on Pt{110}-(1 × 2)[40,41] the surface species that result from methane dissociation,[42,43] and their oxidation[44,45] has been studied. Ethane is the simplest model for studying catalytic reactions involving saturated molecules with carbon−carbon bonds. Our report of the dissociation dynamics of ethane on Pt{110} at low C_2H_6 translational energies appears elsewhere.[46] Here, we identify the surface products of ethane dissociation on Pt{110}-(1 × 2) in the surface temperature range 350−600 K and show that pure species, rather than a mixture, are formed. We also examine the coverage dependence of ethane adsorption and show that a marked change in the character of the adsorbed products occurs at elevated surface temperatures.

2. Experimental Section

The experimental apparatus is described in detail elsewhere.[47] The sample is mounted centrally on a manipulator in an ultrahigh vacuum chamber with a base pressure of $<1 \times 10^{-10}$ mbar. The molecular beam, a supersonic expansion from a 50 μm nozzle, is skimmed, differentially pumped and collimated before entering the sample chamber. An inert King and Wells (KW) flag just in front of the crystal is used to control the dosing time and measure sticking probabilities.[48] The surface temperature (T_s) is monitored by a crystal-mounted thermocouple and is regulated by programmed resistive heating. The partial pressure of gases is monitored using a quadrupole mass spectrometer (QMS) situated behind the crystal. The Pt sample, 11 mm diameter × 1 mm thick, was cut and polished to within 1° of the {110} plane. Initial cleaning of the crystal was achieved by repeated cycles of ion sputtering, annealing, and oxygen treatment. Routine cleaning consisted of annealing at 1240 K, exposure to oxygen for 5 min while cooling from 1100 to 950 K and annealing for 15 min at 950 K. This procedure yields a clean Pt{110}-(1 × 2) surface which gives a sharp LEED pattern and oxygen thermal desorption spectra that are in good agreement with the literature.[49] The C_2H_6 and O_2 used were >99.95% and >99.998% pure, respectively, as quoted by the suppliers (Messer Ltd., U.K.). The ethane molecular beams used for all these experiments were seeded to a composition of 10% C_2H_6 and 90% He and directed along the surface normal. The nozzle temperature was 780 K, giving the ethane molecular beam a translational energy of 78 kJ mol^{-1} calculated on the basis of an ideal supersonic expansion. After each experiment, residual carbon was removed from the surface by oxidation with an O_2 molecular beam at $T_s = 800$ K. The surface was then heated to 1200 K and cooled slowly (1 K s^{-1}) to 600 K to ensure the surface remained well-ordered.

* To whom the correspondence should be addressed. E-mail: dak10@cam.ac.uk.
[†] University of Cambridge.
[‡] University of Washington.

10.1021/jp045441+ CCC: $30.25
Published on Web 02/16/2005

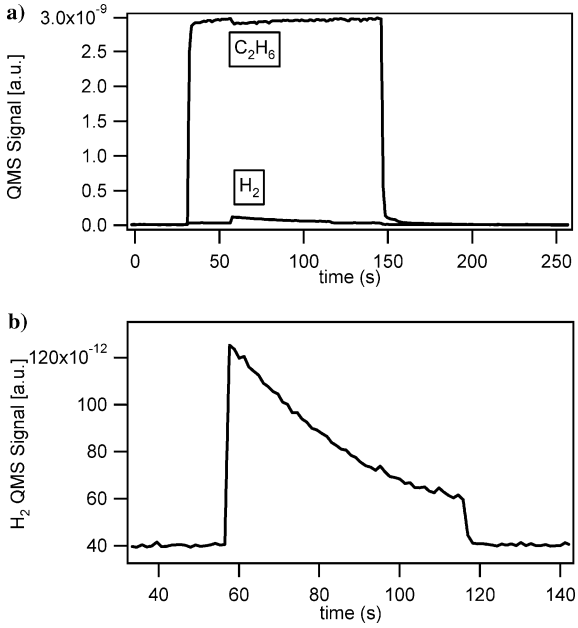

Figure 1. (a) Dissociation of ethane with an incident energy of 78 kJ mol^{-1} on Pt{110} at $T_s = 600$ K. (b) An enlargement of H_2 partial pressure during ethane adsorption. C−H dissociation gives rise to immediate recombinative H_2 desorption from the surface.

3. Results and Discussion

3.1. Ethane Dissociation at $T_s = 600$ K. When ethane dissociative adsorption takes place on Pt{110}, C−H bonds are broken, and coadsorbed C_2H_x and H_a are formed. Above the temperature for recombinative desorption of H_a, 300 K, it immediately desorbs as H_2. A representative ethane dissociation experiment at $T_s = 600$ K is shown in Figure 1a. At $t = 40$ s, an ethane molecular beam enters the UHV chamber and is scattered by the inert KW flag, causing an instantaneous increase in the C_2H_6 partial pressure. At $t = 60$ s, the KW flag is opened, and the ethane beam strikes the platinum surface. A fraction of the impinging molecules dissociate, leading to a drop in the pressure of ethane in the chamber. However, the initial sticking probability of ethane is low (0.03) and difficult to measure accurately using the ethane signal. At $t = 120$ s, the KW flag is closed and no further adsorption takes place. As dissociation begins and the C_2H_6 pressure drops, there is a simultaneous rise in the hydrogen partial pressure, as newly formed surface hydrogen atoms recombine and desorb as H_2. At 600 K, dissociation leads to complete dehydrogenation of the hydrocarbon: all of the C−H bonds are broken and the hydrogen desorbs into the gas phase, leaving only adsorbed carbon on the surface. Thus, no further H_2 desorption is seen when the surface is subsequently heated to temperatures as high as 1200 K.

Figure 1b shows an enlargement of the H_2 signal during the dissociation experiment. The signal has a flat baseline and contains very little noise. This can be used to measure the dissociative sticking probability, $s(t)$, of ethane with great accuracy.[42,46] The carbon species coverages were determined by titration with an oxygen molecular beam at a surface temperature of 800 K, where $CO_{(g)}$ is the sole carbon oxidation product.[50] The integrated area under the CO curve is taken as a measure of the carbon coverage for a particular exposure. At all coverages and at all surface temperatures, the total amount of H_2 produced was directly proportional to the total amount of CO obtained during the subsequent oxidation of adsorbed carbon. This offered additional confirmation that the H_2 signal provides a quantitative measurement of the ethane sticking probability and coverage.

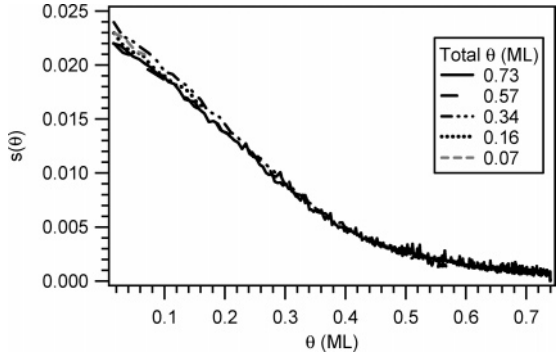

Figure 2. Dissociation probability as a function of ethane coverage at a surface temperature of 600 K.

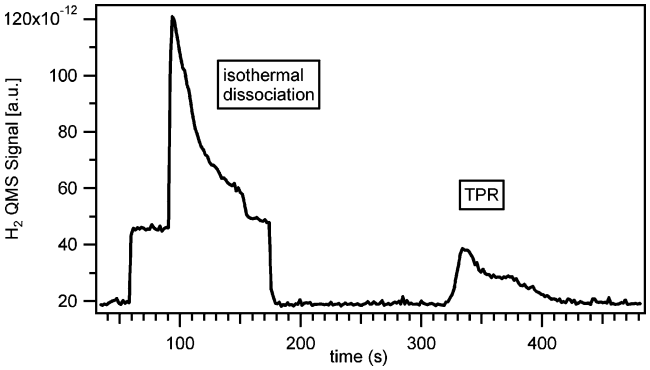

Figure 3. H_2 evolution during isothermal dissociation of ethane at $T_s = 370$ K, followed by temperature-programmed decomposition of the surface hydrocarbon.

3.2. Coverage Dependence of C_2H_6 Dissociation. Throughout this paper, θ will refer to the coverage of C_2H_x ($x = 6-0$) relative to the (1×2) unit cell, i.e., the number of C_2H_x species per unit area divided by 4.6×10^{14}/cm^2. For convenience, we give θ the units of ML, for monolayers, relative to the (1×2) lattice. For example, a coverage of 0.5 ML corresponds to one C_2H_x moiety for every two {110}-(1×2) unit cells. As explained in section 3.6, when the surface is heated to high temperatures (800 K), the surface C_2H_x species is converted to a higher density carbon (C_a) adlayer. However, we will also describe the coverage of this high-temperature carbon in terms of the C_2H_x from which it is formed, using the same coverage scale.

The sticking probability as a function of surface carbon coverage for ethane exposures of fixed beam flux for varying times (final coverages) at $T_s = 600$ K is shown in Figure 2. Once the carbon coverage reaches approximately 0.4 ML, the sticking probability falls much more slowly with increasing coverage. We did not find a "saturation coverage", beyond which no further C_2H_6 dissociation can take place: even for very long exposures, adsorption is found to continue at a finite rate. Our longest exposure of 20 min at 600 K was found to produce a surface carbon coverage of 1.27 ML.

3.3. Stoichiometry and Thermal Stability of the Products of C_2H_6 Dissociation. At surface temperatures less than 600 K, ethane dissociation leads to a partially hydrogenated C_2H_x surface species. The stoichiometry of the stable surface species depends on surface temperature, where the number of H atoms lost per C_2H_6 increases from 4 to 6 in the temperature range 350−600 K.

A typical dissociation experiment at 370 K is shown in Figure 3. At $t = 60$ s, there is a rise in the H_2 partial pressure as a very high-flux ethane molecular beam enters the UHV chamber. This increase is not a result of hydrogen formation at the crystal: it

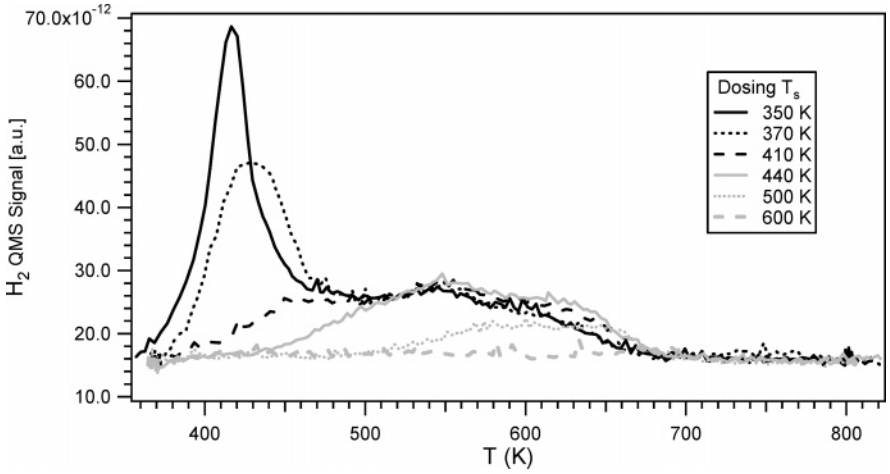

Figure 4. H_2 evolution during temperature-programmed decomposition of surface hydrocarbons formed from ethane dissociation at different surface temperatures. For those experiments where the dissociation temperature was higher than 370 K, the surface was cooled to 370 K immediately after dissociation was complete, before the TPR.

stems entirely from the cracking of C_2H_6 in the mass spectrometer, since the path of the molecular beam to the crystal is blocked by the KW flag. At $t = 90$ s, the flag is opened, and dissociative adsorption commences, giving the sudden increase in the H_2 signal. Dissociation continues until $t = 150$ s, when the KW flag is closed; subsequently, at $t = 180$ s, the molecular beam is turned off. At this point, a surface hydrocarbon with stoichiometry C_2H_x has been prepared. Next, the C_2H_x adlayer is decomposed in a temperature-programmed reaction (TPR) in which the surface is heated at a constant rate of 3 K s^{-1}. The temperature ramp begins at $t = 300$ s, and at $t = 310$ s the formation of H_2 begins. Since the surface temperature at the beginning of the temperature ramp, 370 K, is significantly higher than the peak temperature for H_a recombinative desorption (310 K), gas-phase H_2 must result from a surface reaction in which H_a is produced, namely the decomposition of the surface hydrocarbon fragment via H adatoms.

Ethane exposures (3 min) on clean Pt{110}-(1 × 2) were carried out at different surface temperatures. Figure 4 shows the evolution of H_2 (the only gaseous product) during the subsequent temperature ramps. In each case, the surface temperature was lowered to 370 K as soon as the exposure had ended (except in the experiments where the dissociation itself was performed at 350 or 370 K, and it was not necessary to lower the temperature). Then, in each case, a TPR was run to $T_s = 800$ K at 3 K s^{-1}. For the lowest dissociation temperatures, 350 and 370 K, it is seen that the decomposition of the C_2H_x fragment takes place in two steps. The first is characterized by a sharp peak with a temperature of 430 K, whereas the second is a broader peak with an approximate maximum of 540 K. However, hydrogen formation during the TPR continues until 700 K. This suggests a process in which stepwise dehydrogenation of the surface species occurs: one loss occurs at 430 K, whereas the second takes place with a peak temperature of 540 K but over a broad temperature range.

$$C_2H_x \xrightarrow{430K} C_2H_{x-y} + \frac{y}{2}H_{2(g)} \xrightarrow{540K} 2C + \frac{x-y}{2}H_{2(g)} \quad (1)$$

The stoichiometry of the surface species can be accurately determined by comparing the peak areas for hydrogen evolved during dissociation and during the subsequent TPR. The peak areas were added together to determine the total amount of H_2 produced, and hence, the total amount of C_2H_6 which dissociated. Since each ethane molecule contains six hydrogen atoms, the fractions were multiplied by six to show the number of H atoms per ethane molecule that were released during each step.

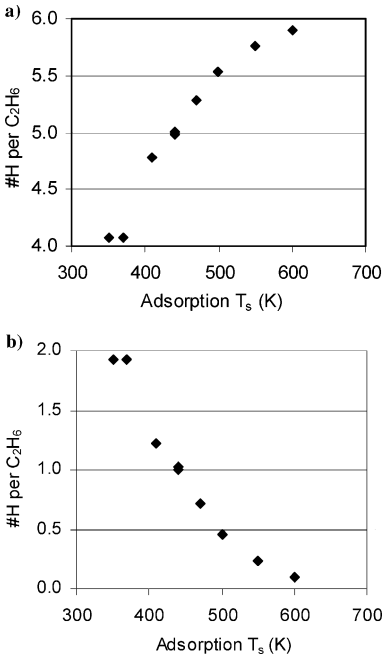

Figure 5. Number of hydrogen atoms evolved (a) during C_2H_6 dissociation and (b) when the resultant surface hydrocarbon is decomposed during a temperature ramp, as a function of the surface temperature during ethane exposure.

The results, in Figure 5, show that at 350 and 370 K four H atoms desorb during dissociative adsorption, whereas a further two desorb during the TPR. This shows that at $T_s = 370$ K the stoichiometry of the surface product is C_2H_2. As the surface temperature is increased, the stable surface product of dissociation changes. At $T_s = 440$ K, five H atoms desorb during the dissociation experiment, and the sixth is removed from the surface hydrocarbon during the TPR, giving net C2H stoichiometry. At higher temperatures, the C2H species also decomposes, and by $T_s = 600$ K, 98% of the hydrogen desorbs as dissociation is taking place. The stoichiometry can be described as follows:

$$C_2H_{6(g)} \xrightarrow{T_s \leq 350K} C_2H_2 + 2H_{2(g)} \xrightarrow{430K} C_2H + \frac{1}{2}H_{2(g)} \xrightarrow{540K} 2C + \frac{1}{2}H_{2(g)} \quad (2)$$

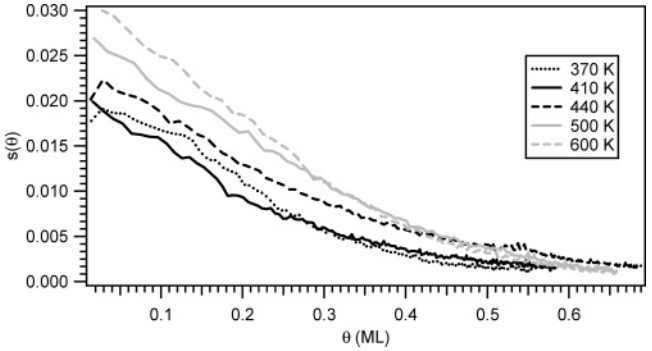

Figure 6. Sticking probability as a function of C_2H_x coverage for ethane dissociation in the surface temperature range 370−600 K.

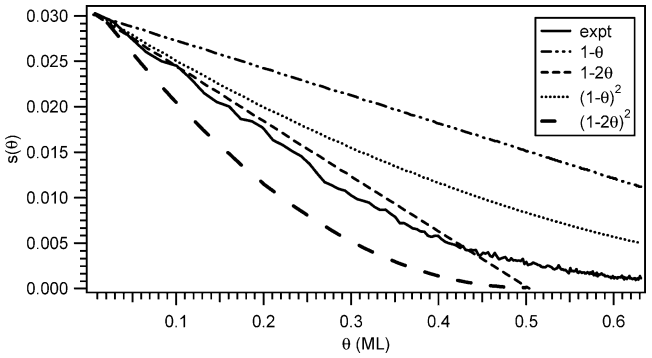

Figure 7. Dissociation probability as a function of surface coverage for C_2H_6 on Pt{110}, $T_s = 600$ K with adsorption behavior predicted by Langmurian models.

3.4. Dissociative Adsorption Mechanism. With the stoichiometry of the ethane dissociation products at different surface temperatures established, it is possible to determine both the sticking probability of C_2H_6 at different T_s and the coverage of the resultant surface products. The sticking probability of ethane as a function of C_2H_x coverage for a series of experiments in the surface temperature range 370−600 K was determined as in section 3.1. The results are shown in Figure 6. In each case, the sticking probability decreases approximately linearly with coverage, until $\theta = 0.4$ ML. Beyond this point, the decrease in s(θ) becomes less pronounced. At 370 and 410 K, the initial sticking probability, s_0, is 0.020. As the surface temperature increases, the sticking probability increases to 0.030 at 600 K. The increase in s_0 with T_s is readily understood in terms of a thermal roughening model [51,52] which predicts that s_0 will vary as $T_s^{1/2}$, similar to the increase in the sticking probability that is observed. The $s(\theta)$ profiles at all surface temperatures are much alike, converging on the same value of 2×10^{-3} when $\theta > 0.5$ ML. This demonstrates that the adsorption mechanism is the same at all surface temperatures and hence for all surface species, in the T_s range studied.

In Figure 7, the sticking probability of ethane at 600 K as a function of the surface species coverage is plotted along with several adsorption profiles predicted by the Langmuir model of adsorption

$$s(\theta) = s_0(1 - a\theta)^n \qquad (3)$$

where a is the number of adsorption sites on a surface filled when a molecule adsorbs and n is the number of sites required. (Throughout this paper, "site" refers to the (1 × 2) lattice.) The experimental data are well described by a (1−2θ) fit up to a coverage of 0.4 ML. The $s(\theta)$ results for ethane dissociation at lower surface temperatures, as shown in Figure 6, were also well fitted with a (1−2θ) function up to 0.4 ML. Above this coverage, the (1−2θ) fit tends to zero while dissociation continues at a finite rate. This indicates an adsorption mechanism described by King and Wells,[48] where a double-spaced structure forms, two empty (1 × 2) sites are required for dissociation, and repulsive lateral interactions lead to short range order in the chemisorbed overlayer. If the adlayer were completely ordered, the sticking probability would be 0 at $\theta = 0.5$ ML. However, since the adlayer does contain some disorder, at coverages higher than 0.5 ML adsorption can continue to take place. This result is consistent with studies of the CH species on Pt{110}-(1 × 2),[43] where at saturation coverage there was one CH fragment present for every two (1 × 2) unit cells: the CH species was observed to form a c(2×4) overlayer.

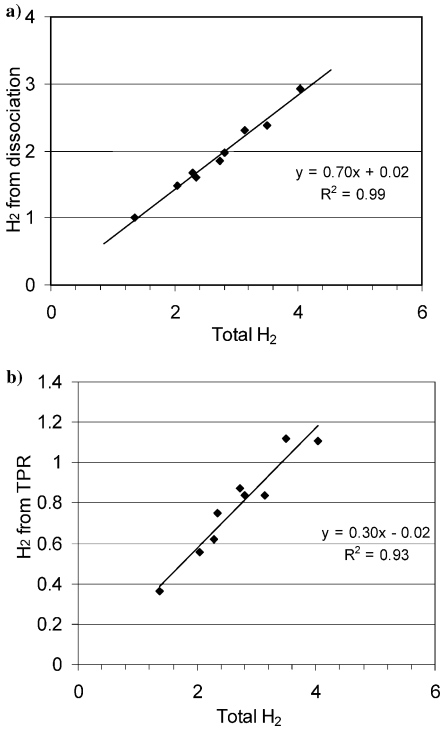

Figure 8. (a) Fraction of the total H_2 in ethane molecule that desorbs during dissociative adsorption at 370 K. (b) The fraction of H_2 that desorbs upon heating after dissociative adsorption at 370 K.

3.5. Stable Surface C_2H_x Products: C_2H_2 and C_2H. In section 3.3, it was shown that the stoichiometry of the surface species formed from ethane dissociation was C_2H_2 at $T_s = 370$ K and C_2H at $T_s = 440$ K. However, several types of surface species could give rise to this stoichiometry, including $(C_2H_2)_n$ or $(C_2H)_n$ clusters, or a mixture of species. For example, coadsorbed C_2H_3 and C_2H might have an average stoichiometry of C_2H_2. We now present evidence that C_2H_2 and C_2H are in fact the molecular formulas of the surface species and that pure adlayers of these species are generated at all surface coverages. First, the TPR profiles for the surface species produced at $T_s = 370$ K were examined, for nine different experiments where the surface coverage was varied in the range 0.18−0.54 ML. For each experiment, the total amount of H_2 evolved during both dissociation and the TPR was determined by adding together the hydrogen peak areas from each step. The fractions of the total hydrogen that desorb during dissociation and during the TPR are shown in Figure 8. For both the dissociation and the TPR steps, the fraction of the total H_2 evolved is constant as a function of coverage: 70% of the hydrogen is obtained during dissociation, the remaining 30% during thermal decom-

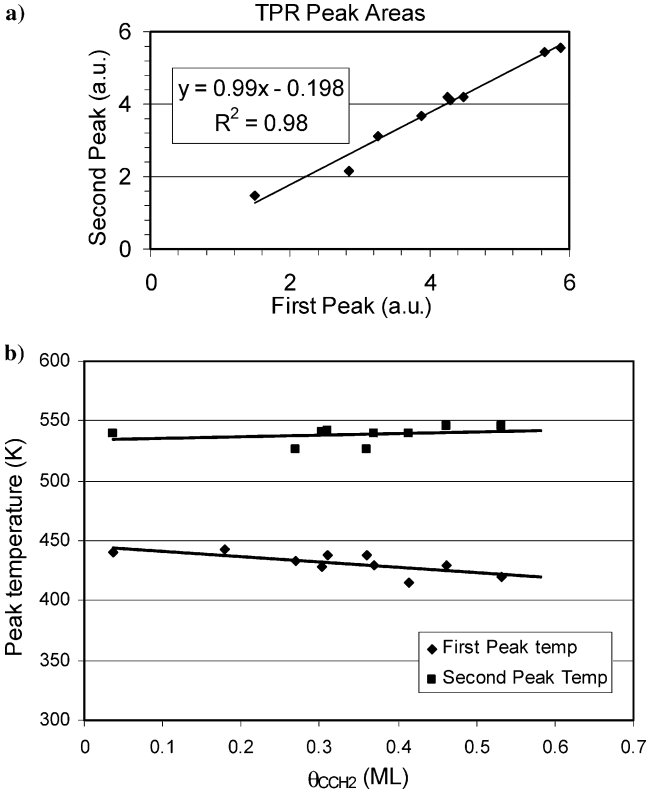

Figure 9. (a) Areas of the two TPR peaks when CCH_2 overlayers of varying coverage are prepared at 370 K and heated. (b) The peak temperature positions for the TPR of CCH_2 adlayers of varying coverages prepared at 370 K.

position. Clearly, the stoichiometry of the surface species is C_2H_2 throughout the C_a coverage range 0.18−0.54 ML at 370 K.

The fact that the surface stoichiometry is C_2H_2 over a wide coverage range strongly suggests that there is a single surface product rather than a mixture. If a mixture of species were formed, one would expect the more dehydrogenated one to predominate at low coverages. At higher coverages, where fewer surface sites were available for C−H bond cleavage, a species with more H atoms per C atom would form. In this case, H_2 that was produced during dissociation would not be linear with coverage but would be much larger at low coverages. It also argues against carbon−carbon bond formation, which has been observed between CH_3 groups on Pt{111},[38,53] since one would expect such bonding to be accompanied by the weakening or breaking of C−H bonds. In this scenario, one would expect the fraction of the hydrogen that desorbed during dissociation to be greater at high coverages, where C−C bond formation would be more probable.

Further results, which suggest that a pure species is formed, and that C−C coupling does not occur, are found in Figure 9a. Here the areas of the two H_2 peaks observed during thermal decomposition of the surface hydrocarbon are compared and found to be equal at all coverages. If a mixture of species were present, at low coverage, one would expect very little H_2 at all in the low-temperature peak. At high coverages, the low-temperature peak would contain much more hydrogen than the second peak. Similarly, carbon−carbon coupling would be almost certain to alter the bonding in the C_2H_2 species. Figure 9b shows the temperatures of the two peak maxima during the TPR. In the CCH_2 coverage range 0.18−0.54 ML, both peak temperatures are constant with coverage to within 20 K. Once again, constant peak temperatures are consistent with the decomposition of a single surface species and inconsistent with a mixture of C_2 species or carbon−carbon coupling. Taken collectively, the points discussed above make it almost certain that ethane dissociation leads to a single surface product at 350−400 K, CCH_2, and that carbon−carbon coupling does not occur for C_a coverages as high as 0.55 ML.

The possibility of C−C bond cleavage to produce either C_a and CH_{2a} or $2CH_a$ has not been considered. However, this possibility can be ruled out based on the work of the studies of methane dissociation on Pt{110} by Watson et al.[43,54] It was found that the only stable surface product of CH_4 dissociation was CH. Therefore, if C−C bond breaking led to the formation of $C_a + CH_2$, the latter would immediately decompose to the more stable CH species. Moreover, when a CH adlayer was exposed to a deuterium molecular beam, it exchanged readily with D_a and could be rehydrogenated to CD_4 and CHD_3 under conditions of an intense D_2 flux.[54] In contrast, although exposure of C_2H_2 adlayers to extremely high flux D_2 molecular beams led to incomplete deuterium exchange with the surface hydrocarbon, it resulted in the formation of no gas-phase C_1 or C_2 hydrocarbons.

With the possibility of C−C bond cleavage excluded, the surface product of C_2H_6 dissociation at $T_s = 370$ K must be C_2H_2. This species thermally decomposes with a peak temperature of 430 K to yield C_2H, which in turn decomposes above 500 K to give surface carbon. The C_2H_2 species has been observed on Pt{110} before. Yagasaki et al. studied ethylene thermal decomposition on Pt{110}-(1×2) using HREELS[31] and identified a mixture of C_2H_2 and C_2H_3 at $T_s = 300$ K. The CH_2 wag and scissors modes were observed at 990 and 1420 cm^{-1}, respectively, showing that the surface species was in fact CCH_2 and not HCCH. Moreover, the C−C stretch frequency was 1130 cm^{-1}. This is much less than for the upright vinylidene species on Pt{110}-(1×1), where the CH_2 carbon did not interact with the surface and the C−C stretch frequency was 1585 cm^{-1}.[32] Therefore, the CH_2 carbon must be bonded to the surface. The proportion of CCH_2 relative to CCH_3 was higher at lower coverages, as one would expect for an adlayer containing a mixture of species. Stuck et al. conducted a calorimetry study of ethylene adsorption on Pt{110}-(1 × 2) at $T_s = 300$ K[33] and found that C_2H_2 is formed at very low surface coverages. Once again, however, at higher coverages the surface products were the more fully hydrogenated species CCH_3 and C_2H_4.

In the current work, only CCH_2 is observed. However, it is important to note that surface temperatures 300 K or less are not sufficient to completely desorb H_a. Coadsorbed hydrogen has previously been shown to inhibit the decomposition of $CHCH_3$ to CCH_3 on Pt{111}. Conversion of a pure C_2H_4 adlayer, via a $CHCH_3$ intermediate takes place at surface temperatures of 230−250 K,[19,24] whereas in the presence of coadsorbed H_a, conversion only takes place once $T_s > 300$ K, when H_a has desorbed. At $T_s = 370$ K, H_a desorbs as H_2 as soon as it forms, and the product of C_2H_6 dissociation is a pure CCH_2 adlayer, at all surface coverages.

3.6. High-Density Carbon Layer at $T_s = 800$ K. When the surface temperature is increased from 600 to 800 K, the coverage dependence of ethane dissociation changes dramatically. As shown in section 3.4, the dependence of the dissociation probability of ethane on the coverage of the surface species is very similar for all surface temperatures in the range 370−600 K. However, at $T_s = 800$ K, the dependence of sticking on θ is entirely different. In Figure 10, the H_2 formation rates (i.e., the H_2 signal) versus the resulting C coverage during exposures of the initially clean Pt surface to a C_2H_6 beam at surface temperatures of 600 and 800 K are shown. It is seen that the

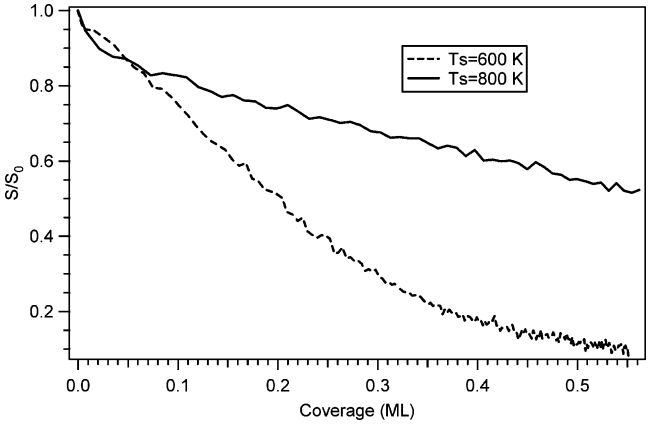

Figure 10. Sticking probability during the dissociative adsorption of C_2H_6 at 600 K (dashed line) and 800 K (solid line) plotted versus the resulting carbon coverage deposited on the surface.

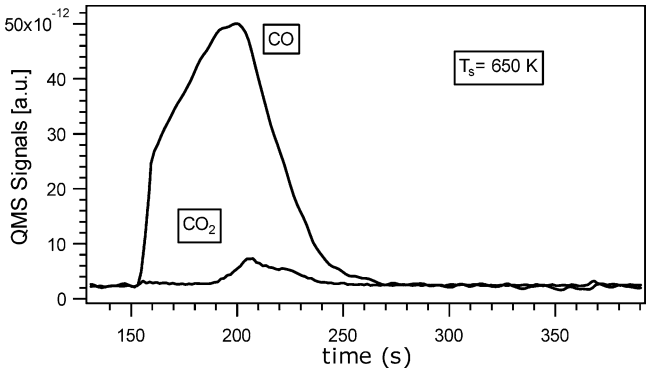

Figure 11. Oxidation of 0.35 ML C_2 with an oxygen molecular beam (turned on at $t = 155$ s) to form CO and CO_2. The C_2 species was formed from ethane dissociation at a temperature of 600 K; the oxidation takes place at 650 K. The reactive adsorption of O_2 on the surface is not shown.

initial sticking probability is almost identical for the two experiments. However, at $\theta = 0.5$ ML, the sticking probability at 600 K has decreased to approximately 10% of its initial value, whereas at 800 K, the sticking probability has decreased far more slowly, remaining at ~60% of the initial value. A 5-min exposure of ethane at $T_s = 800$ K (not shown) yields a surface carbon coverage of 1.45 ML, whereas the sticking probability remains relatively high (3×10^{-3}). Clearly, the $(1-2\theta)$ dependence of $s(\theta)$ has changed above 600 K. We attribute this change to the agglomeration of C_a into high-density islands by 800 K. This is consistent with the finding of Janin et al., who observed the formation of graphite overlayers on Pt{110}-(1×2) when the surface was annealed in ethylene at surface temperatures above 870 K.[55]

3.7. Oxidation Kinetics of the Carbon Adlayer. In Figure 11, a 0.38 ML carbon adlayer prepared by ethane dissociation at 600 K is oxidized to CO and CO_2 using an oxygen molecular beam, at a surface temperature of 650 K. We show in section 3.1 that C_2H_6 dissociation at 600 K gives rise to a carbon adlayer. As can be seen, 90% of this carbon is oxidized to form CO gas, and the remainder is oxidized completely to CO_2. Watson et. al. have shown previously that CH_4 dissociation at 600 K gives rise to a hydrogen-free carbon layer, which we will refer to as "C_a" without meaning by this any implication with respect to C−C bonding of lack thereof.[43] The oxidation profile of a similar coverage of that C_a species at 650 K[44] is very similar to the reaction profile for the surface carbon shown in Figure 11. This suggests that the same C_a species is being produced here. As the oxidation temperature is increased above 650 K, the selectivity of that $C_a + O_2$ reaction for CO rather than CO_2 increased, with approximately 99% of the surface carbon forming CO at 750 K.[50] We see the same for the carbon produced from ethane at these temperatures, which again suggests that the same form of surface carbon is produced here as from methane.[50]

We showed in Figure 10 that the surface carbon formed during ethane dissociation at $T_s = 800$ K is different from that which is prepared at 600 K. When a carbon adlayer made by ethane dissociation at 800 K is titrated at 650 K as in Figure 11, the oxidation kinetics were also observed to be markedly different. This again highlights the difference in the structure of the C_a formed from ethane at 800 K, compared to 650 K.

The discovery of an adsorption regime in which ethane dissociation leads to a high density carbon layer with higher than expected reactivity to oxygen, at catalytically important surface temperatures, is significant. Results of investigations into the nature of the carbon formed on the surface at this temperature, the maximum C_a coverage that can be obtained, and the reactivity of this carbon to oxygen will be published in a forthcoming paper.[56]

4. Summary and Conclusion

The adsorption and surface products of ethane on Pt{110}-(1 × 2) have been studied using high-flux supersonic molecular beams and temperature-programmed reaction techniques. At surface temperatures of 350−400 K, a single surface product, CCH_2, is formed. The CCH_2 species thermally decomposes in a stepwise process to form CCH at 440 K, and C_{2a} (or 2 C) at $T_s \geq 600$ K. At $T_s \geq 800$ K, C_2H_6 dissociation leads to the formation of a high-density carbon layer.

The sensitivity to the surface temperature of the dissociation products of ethane on Pt{110} demonstrates that the selectivity of catalytic reactions involving surface hydrocarbons can vary significantly with surface temperature; it also illustrates the importance of properly characterizing the surface species that are expected in catalytic reactions over a wide temperature range.

Acknowledgment. We acknowledge the EPRSC for an equipment grant and postdoctoral support (V.F.), Shell Global Solutions B.V. and the Cambridge Commonwealth Trust for a research studentship (J.J.W.H), and DOE-BES for support (C.T.C).

References and Notes

(1) Horiuti, I.; Polanyi, M. *Trans. Faraday Soc.* **1934**, *30*, 1164−1172.
(2) Bodke, A. S.; Olschki, D. A.; Schmidt, L. D.; Ranzi, E. *Science* **1999**, *285*, 712−715.
(3) Dry, M. E. *Catal. Today* **2002**, *71*, 227−241.
(4) Rostrup-Nielsen, J. R. *Catal. Today* **2000**, *63*, 159−164.
(5) Hung, W. H.; Bernasek, S. L. *Surf. Sci.* **1995**, *339*, 272−290.
(6) Bhattacharya, A. K.; Pyke, D. R. *J. Mol. Catal. A-Chem.* **1998**, *129*, 279−285.
(7) Papageorgopoulos, D. C.; Ge, Q.; Nimmo, S.; King, D. A. *J. Phys. Chem. B* **1997**, *101*, 1999−2005.
(8) Mate, C. M.; Kao, C. T.; Bent, B. E.; Somorjai, G. A. *Surf. Sci.* **1988**, *197*, 183−207.
(9) Jungwirthova, I.; Kesmodel, L. L. *J. Phys. Chem. B* **2001**, *105*, 674−680.
(10) Hills, M. M.; Parmeter, J. E.; Mullins, C. B.; Weinberg, W. H. *J. Am. Chem. Soc.* **1986**, *108*, 3554−3562.
(11) Henderson, M. A.; Mitchell, G. E.; White, J. M. *Surf. Sci.* **1988**, *203*, 378−394.
(12) Livneh, T.; Asscher, M. *J. Phys. Chem. B* **2000**, *104*, 3355−3363.
(13) Parlett, P. M.; Chesters, M. A. *Surf. Sci.* **1996**, *357*, 791−795.
(14) Hutson, F. L.; Ramaker, D. E.; Koel, B. E.; Gebhard, S. C. *Surf. Sci.* **1991**, *248*, 119−133.

(15) Zhu, X.-Y.; Castro, M. E.; Akhter, S.; White, J. M.; Houston, J. E. *Surf. Sci.* **1988**, *207*, 1−16.
(16) Carter, E. A.; Koel, B. E. *Surf. Sci.* **1990**, *226*, 339−357.
(17) Steininger, H.; Ibach, H.; Lehwald, S. *Surf. Sci.* **1982**, *117*, 685−698.
(18) Yata, M.; Madix, R. J. *Surf. Sci.* **1995**, *328*, 171−180.
(19) Land, T. A.; Michely, T.; Behm, R. J.; Hemminger, J. C.; Comsa, G. *J. Chem. Phys.* **1992**, *97*, 6774−6783.
(20) Erley, W.; Li, Y.; Land, D. P.; Hemminger, J. C. *Surf. Sci.* **1994**, *301*, 177−196.
(21) Yeo, Y. Y.; Stuck, A.; Wartnaby, C. E.; King, D. A. *Chem. Phys. Lett.* **1996**, *259*, 28−36.
(22) Starke, U.; Barbieri, A.; Materer, N.; Van Hove, M. A.; Somorjai, G. A. *Surf. Sci.* **1992**, *286*, 1−14.
(23) Zaera, F.; Janssens, T. V. W.; Ofner, H. *Surf. Sci.* **1996**, *368*, 371−376.
(24) Cremer, P. S.; Su, X.; Shen, Y. R.; Somorjai, G. A. *J. Am. Chem. Soc.* **1996**, *118*, 2942−2949.
(25) Ohtani, T.; Kubota, J.; Kondo, J. N.; Hirose, C.; Domen, K. *Surf. Sci.* **1998**, *415*, 983−987.
(26) Ofner, H.; Zaera, F. *J. Phys. Chem. B* **1997**, *101*, 396−408.
(27) Zaera, F. *J. Phys. Chem.* **1990**, *94*, 5090−5095.
(28) Janssens, T. V. W.; Zaera, F. *Surf. Sci.* **1995**, *344*, 77−84.
(29) Zaera, F. *J. Phys. Chem.* **1990**, *94*, 8350−8355.
(30) Zaera, F.; French, C. R. *J. Am. Chem. Soc.* **1999**, *121*, 2236−2243.
(31) Yagasaki, E.; Backman, A. L.; Masel, R. I. *J. Phys. Chem.* **1990**, *94*, 1066−1072.
(32) Yagasaki, E.; Masel, R. I. *J. Am. Chem. Soc.* **1990**, *112*, 8746−8750.
(33) Stuck, A.; Wartnaby, C. E.; Yeo, Y. Y.; King, D. A. *Phys. Rev. Lett.* **1995**, *74*, 578−581.
(34) Weaver, J. F.; Carlsson, A. F.; Madix, R. J. *Surf. Sci. Rep.* **2003**, *50*, 107−200.
(35) McMaster, M. C.; Madix, R. J. *Surf. Sci.* **1992**, *275*, 265−280.
(36) McMaster, M. C.; Madix, R. J. *J. Chem. Phys.* **1993**, *98*, 9963−9976.
(37) Oakes, D. J.; Newell, H. E.; Rutten, F. J. M.; McCoustra, M. R. S.; Chesters, M. A. *Chem. Phys. Lett.* **1996**, *253*, 123−128.
(38) Oakes, D. J.; Newell, H. E.; Rutten, F. J. M.; McCoustra, M. R. S.; Chesters, M. A. *J. Vac. Sci. Technol. A* **1996**, *14*, 1439−1447.
(39) Newell, H. E.; McCoustra, M. R. S.; Chesters, M. A.; De La Cruz, C. *J. Chem. Soc. Faraday Trans.* **1998**, *94*, 3695−3698.
(40) Walker, A. V.; King, D. A. *J. Chem. Phys.* **2000**, *112*, 4739−4748.
(41) Walker, A. V.; King, D. A. *Phys. Rev. Lett.* **1999**, *82*, 5156−5159.
(42) Watson, D. T. P.; van Dijk, J.; Harris, J. J. W.; King, D. A. *Surf. Sci.* **2002**, *506*, 243−250.
(43) Watson, D. T. P.; Titmuss, S.; King, D. A. *Surf. Sci.* **2002**, *505*, 49−57.
(44) Watson, D. T. P.; Harris, J. J. W.; King, D. A. *J. Phys. Chem. B* **2002**, *106*, 3416−3421.
(45) Watson, D. T. P.; Harris, J. J. W.; King, D. A. *Surf. Sci.* **2002**, *505*, 58−70.
(46) Harris, J. J. W.; Laffir, F. R.; Fiorin, V.; King, D. A. *Surf. Sci. Lett.* Submitted.
(47) Hopkinson, A.; Guo, X. C.; Bradley, J. M.; King, D. A. *J. Chem. Phys.* **1993**, *99*, 8262−8279.
(48) King, D. A.; Wells, M. G. *Proc. Royal Soc. London A* **1974**, *339*, 245−269.
(49) Walker, A. V.; Klotzer, B.; King, D. A. *J. Chem. Phys.* **1998**, *109*, 6879−6888.
(50) Walker, A. V.; King, D. A. *J. Chem. Phys.* **2000**, *112*, 1937−1945.
(51) Pasteur, A. T.; Dixon-Warren, S. J.; Ge, Q.; King, D. A. *J. Chem. Phys.* **1997**, *106*, 8896−8904.
(52) Luntz, A. C. *J. Chem. Phys.* **1995**, *102*, 8264−8269.
(53) Fairbrother, D. H.; Peng, X. D.; Trenary, M.; Stair, P. C. *J. Chem. Soc. Faraday Trans.* **1995**, *91*, 3619−3625.
(54) Watson, D. T. P.; Ge, Q.; King, D. A. *J. Chem. Phys.* **2001**, *115*, 11306−11316.
(55) Janin, E.; Gothelid, M.; Karlsson, U. O. *Appl. Surf. Sci.* **2000**, *162*, 184−189.
(56) Laffir, F. R.; Harris, J. J. W.; Fiorin, V.; King, D. A. *J. Chem. Phys.* To be submitted.